Many-hole interactions and the average lifetimes of chaotic transients that precede controlled periodic motion

Buljan, Hrvoje; Paar, Vladimir

Many-hole interactions and the average lifetimes of chaotic transients that precede controlled periodic motion

Hrvoje Buljan and Vladimir Paar
Department of Physics, Faculty of Science, University of Zagreb, 10000 Zagreb, Croatia
(Received 15 December 2000; published 15 May 2001)

We consider n small regions (referred to as the holes) on a chaotic attractor and study the average lifetime it takes for a randomly initiated trajectory to land in their union. The holes are thought of as n possible escape routes for the trajectory. The escape route through one of the holes may be considerably reduced by other holes, depending on their positions. This effect, referred to as shadowing, can significantly prolong the average lifetime. The main result of this paper is the construction and analysis (numerical and theoretical) of the many-hole interactions. They are interpreted as the amount of shadowing between the holes. The ''effective range'' of these interactions is associated with the largest Lyapunov exponent. The shadowing effect is shown to be very large when the holes are located on n points of an unstable periodic orbit. Considerable attention is paid to this case since it is of interest to the field of controlling chaos.

DOI: 10.1103/PhysRevE.63.066205 PACS number(s): 05.45.Gg, 05.45.Ac

I. INTRODUCTION

The average lifetime of chaotic transients is an important physical quantity in the field of controlling chaos [1–9]. Let us briefly disclose this relation. Chaotic attractors are densely populated by unstable periodic orbits [10,11]. In order to improve the system performance, we may desire that a particular unstable periodic orbit becomes stable, i.e., attracting [1–6,12]. Suppose that we monitor a randomly initiated trajectory on a chaotic attractor. Due to ergodicity, the trajectory once in a while lands very close to the desired periodic orbit [1,6,10,11]. When it happens, the trajectory approximately follows the periodic orbit for a few cycles. Thus, during a brief time interval the behavior of the trajectory resembles periodic motion. As time increases, the trajectory moves away from the unstable periodic orbit due to its repelling properties. In Refs. [1–6] it has been demonstrated that the trajectory can be forced to closely follow the unstable periodic orbit for a long time interval by applying only small, time-dependent perturbations in a system parameter. Since these perturbations are small, they are efficient only once the trajectory lands sufficiently close to the desired periodic orbit [1–6]. Therefore, the controlled periodic motion is preceded in time by a chaotic transient.

The theoretical analysis of this work mainly draws upon the connection between the average lifetime and the conditionally invariant measure, also referred to as the c measure [13–20]. The c measures appear in connection with transiently chaotic dynamical systems [13–15]. A rigorous mathematical analysis of these measures can be found in Refs. [17–20], where the existence and uniqueness of the c measures has been established for a broad class of systems.

The problem studied in this paper encompasses the problem of average lifetimes preceding controlled periodic motion. Suppose that a chaotic attractor (A) presents the asymptotic behavior of a one-dimensional (1D) noninvertible or 2D invertible map O: $D \to D$, $D \subseteq \mathbf{R}^m$, $m \in \{1,2\}$. Imagine n small regions $H_i \subset D$, $i=1,2,\ldots,n$, referred to as the holes, that are located on the attractor A. Let the hole $H_i \equiv H_{i,\epsilon}(\boldsymbol{\xi}_i)$ be an m-dimensional ball of radius ϵ centered at a point $\boldsymbol{\xi}_i$. The probability that a trajectory, originating from a point chosen at random (using a uniform probability distribution), does not land within the union of n holes

$$H_{12\cdots n} = H_1 \cup H_2 \cup \cdots \cup H_n \tag{1}$$

during the first t time steps is

$$\sim \exp(-t/\tau^{(n)}_{12\cdots n}), \quad \text{for} \quad t \gg 1, \tag{2}$$

where $\tau^{(n)}_{12\cdots n}$ denotes the average lifetime it takes for a trajectory to land (for the first time) within the set $H_{12\cdots n}$ [1,6,13,21].

Given a map O, the lifetime $\tau^{(n)}_{12\cdots n}$ is a function of the size (ϵ) and the positions of the holes ($\boldsymbol{\xi}_i$). In accordance with Refs. [1,6,8,13,21], the lifetime obeys a typical power-law dependence on ϵ [$\tau^{(n)}_{12\cdots n} \sim \epsilon^{-\gamma}$]. In the present work we analyze the functional dependence of the average lifetime $\tau^{(n)}_{12\cdots n} \equiv \tau^{(n)}(\boldsymbol{\xi}_1, \boldsymbol{\xi}_2, \ldots, \boldsymbol{\xi}_n)$ on the positions of the holes. For a special case when

$$O(\boldsymbol{\xi}_i) = \boldsymbol{\xi}_{i+1}, \quad i=1,\ldots,n, \tag{3}$$

($\boldsymbol{\xi}_{n+1} \equiv \boldsymbol{\xi}_1$), i.e., when the holes are centered on the points of an unstable periodic orbit of prime period n, the lifetime $\tau^{(n)}_{12\cdots n}$ corresponds to average lifetimes of chaotic transients that precede controlled periodic motion [1–6].

Suppose that a trajectory, at the time step t, lands within the set $H_{12\cdots n}$ for the first time. The trajectory has landed in just one of the holes, say H_j. We may think of n holes as n possible landing grounds or escape routes for the chaotic trajectory. At the time step $t-l$ ($l \geqslant 1$), the trajectory was certainly within the set $O^{-l}(H_j)$. Every preimage of H_j can be thought of as the access to H_j. If another hole, say H_i, intersects with $O^{-l}(H_j)$, then H_j can be accessed only through $O^{-l}(H_j) \setminus H_i$ [see Fig. 1(a)]. For some positions of the holes H_i and H_j, H_i can considerably reduce the accessibility to the hole H_j. When this happens, we say that the hole H_i ''casts a shadow'' [22] on the hole H_j [Fig. 1(a)]. If

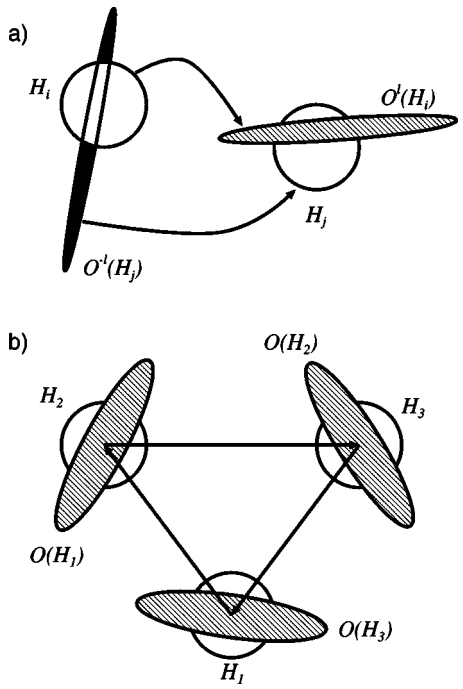

FIG. 1. (a) H_j is accessible only through its preimages, e.g., $O^{-l}(H_j)$. Since $O^{-l}(H_j)\cap H_i\neq\emptyset$, H_j is actually accessible only through $O^{-l}(H_j)\setminus H_i$ (colored black). We say that the hole H_i casts a shadow on the hole H_j. The shadow of H_i is shaded with diagonal lines. (b) Three holes are centered on a periodic orbit of period three. The shadowing effect is extremely large since every hole shadows the next one.

H_j is shadowed by other hole(s), the escape route via H_j is significantly suppressed and the lifetime is prolonged.

We will demonstrate that, as a consequence of the shadowing effect, $\tau^{(n)}_{12\cdots n}$ exhibits sharp peaks for some positions of the holes. The magnitude of a particular peak corresponds to the total amount of shadowing between the holes. For the special case when the holes are centered on the points of an unstable periodic orbit [Eq. (3)], the total amount of shadowing is extremely large. Every hole shadows the next one. H_1 shadows H_2, H_2 shadows H_3, and so on [see Fig. 1(b)]. Hence, in the case of interest for controlling chaos, the average lifetime $\tau^{(n)}_{12\cdots n}$ exhibits one of its most pronounced peaks.

The inverse of the average lifetime is identical to the escape rate, the quantity standardly used for the characterization of transiently chaotic systems [13–15]. In order to investigate the functional dependence $\tau^{(n)}_{12\cdots n}\equiv\tau^{(n)}(\boldsymbol{\xi}_1,\boldsymbol{\xi}_2,\ldots,\boldsymbol{\xi}_n)$, we will decompose the escape rate $1/\tau^{(n)}_{12\cdots n}$ as a sum of the one-hole escape rates $\Sigma^n_{i=1}1/\tau^{(1)}_i$, plus the interference terms that will be referred to as the many-hole interactions. We will demonstrate that the magnitude of the many-hole interactions reflects the amount of shadowing between the holes. The functional dependence $\tau^{(n)}(\boldsymbol{\xi}_1,\boldsymbol{\xi}_2,\ldots,\boldsymbol{\xi}_n)$ can be analyzed by investigating the functional dependence of the many-hole interactions on the positions of the holes. The main result of this paper is the construction, numerical, and theoretical analysis of the many-hole interactions.

It will be demonstrated that for some random choice of the positions $\boldsymbol{\xi}_i$, it is most likely that there will be no shadowing, i.e., the many-hole interactions are $\simeq 0$. We will show that this is a consequence of a very small ''effective range'' of the many-hole interactions. The ''effective range'' of the many-hole interactions will be associated with the positive Lyapunov exponent of the map O. Furthermore, magnitudes of the peaks in the lifetime $\tau^{(n)}_{12\cdots n}$ will be analyzed by studying the corresponding peaks in the many-hole interactions.

The paper is organized as follows. In Sec. II we associate the n-hole lifetime $\tau^{(n)}_{12\cdots n}$ with the conditionally invariant measure. In Sec. III we study the two-hole lifetime $\tau^{(2)}_{12}$ and introduce the concept of the pairwise interaction between the holes. In Sec. IV we study the three-hole lifetime $\tau^{(3)}_{123}$ and introduce the concept of the residual interaction between the holes. In Sec. V we introduce the residual n-hole interaction $\Delta^{(n)}_{12\cdots n}$ and generalize the results. In particular, for the case when the hole positions satisfy Eq. (3), we show that the contribution of the n-hole residual interaction within the decomposition of the escape rate $1/\tau^{(n)}_{12\cdots n}$ decreases exponentially fast with the increase of n. The characteristic exponent is shown to be approximately equal to the positive Lyapunov exponent of the map O.

The one-hole lifetime, say $\tau^{(1)}(\boldsymbol{\xi}_1)$, was phenomenologically studied for the logistic map in Refs. [23,24]. A theoretical explanation of these results was reported in Ref. [7], where it was demonstrated that when H_1 encompasses a point on a short periodic orbit, $\tau^{(1)}(\boldsymbol{\xi}_1)$ significantly deviates from the inverse of the naturally invariant measure (μ_N) contained within H_1, $\mu_N(H_1)^{-1}$. The significance of this deviation was described in terms of the ratio $\tau^{(1)}(\boldsymbol{\xi}_1)/\mu_N(H_1)^{-1}$, which was found to be a function of the unstable eigenvalue of the shortest periodic orbit visiting H_1.

In Sec. VI we generalize the main result from Ref. [7] to the n-hole case. If a given region on a chaotic attractor is visited more frequently by typical trajectories, i.e., if a given region contains a larger amount of naturally invariant measure, the average lifetime it takes for an orbit to land in that region will be smaller. Hence, $\mu_N(H_{12\cdots n})^{-1}$ can be used as an estimate for $\tau^{(n)}_{12\cdots n}$. However, we will demonstrate that when the holes are located on an unstable periodic orbit [Eq. (3)], due to the extremely large shadowing effect, the estimate $\mu_N(H_{12\cdots n})^{-1}$ is significantly smaller than $\tau^{(n)}_{12\cdots n}$. It will be demonstrated that $\tau^{(n)}_{12\cdots n}/\mu_N(H_{12\cdots n})^{-1}$ is a function of the unstable eigenvalue of the unstable periodic orbit.

II. THE AVERAGE LIFETIMES AND THE CONDITIONALLY INVARIANT MEASURES

The concept of shadowing (Fig. 1) pictorially explains significant prolongations of the lifetime $\tau^{(n)}_{12\cdots n}$ that occur for some positions of the holes. However, a more sophisticated treatment of the problem requires the concept of the conditionally invariant measure [13–20].

The c measure is closely associated with an auxiliary modified map [7,18,19,23,24]

$$O_{12\cdots n}(\boldsymbol{\xi}')=\begin{cases} O(\boldsymbol{\xi}'), & \boldsymbol{\xi}'\in D\backslash H_{12\cdots n}, \\ \text{outside of } B, & \boldsymbol{\xi}'\in H_{12\cdots n}, \end{cases} \tag{4}$$

where B denotes the basin of attraction of A. Let $x_0\in B$ be a point chosen at random (using a uniform probability distribution). A trajectory of the original map O originating from x_0 remains on the chaotic attractor forever. A trajectory of the modified map $O_{12\cdots n}$ originating from the same initial condition is exactly the same as for the original map O, but only until it lands within the set $H_{12\cdots n}$. After that moment this trajectory escapes through the region $H_{12\cdots n}$, i.e., it is no longer considered. Therefore, the modified map $O_{12\cdots n}$ is transiently chaotic. The average lifetime of chaotic transients created by the map $O_{12\cdots n}$ is equal to $\tau^{(n)}_{12\cdots n}$, which we have defined above. Similar maps with a forbidden gap region arise in the context of communicating with chaos [25] and in calculation of the topological entropy [26,27]. A broad class of maps with holes and related conditionally invariant measures have been studied in Refs. [17–20].

In the following an operational definition of the c measure is given. The chaotic attractor is covered with cells (call them $C\subset D$) from a very fine grid. Suppose that we uniformly distribute a large number of points (N) in the phase space D. The points are iterated by the modified map $O_{12\cdots n}$ for a large number of time steps (T). Let us observe the surviving points, i.e., the points that have not visited the set $H_{12\cdots n}$ during the first $T-1$ time steps. In the limit $N\rightarrow\infty$, $T\rightarrow\infty$, the fraction of surviving points in a given cell C converges to the c measure [call it $\mu^{(n)}_{C12\cdots n}$] contained within that cell, $\mu^{(n)}_{C12\cdots n}(C)$ [13–15,17–20]. Thus, for a given map O, the conditionally invariant measure $\mu^{(n)}_{C12\cdots n}$ is defined by the set $H_{12\cdots n}$, i.e., by the positions and the size of the holes. The upper and lower indices in μ_C indicate the number of holes and their positions, respectively.

In accordance with Refs. [13,14,17–20], the c measure $\mu^{(n)}_{C12\cdots n}$ satisfies the following relation:

$$\mu^{(n)}_{C12\cdots n}(C)=\exp(1/\tau^{(n)}_{12\cdots n})\mu^{(n)}_{C12\cdots n}(O^{-1}_{12\cdots n}(C)), \tag{5}$$

where

$$O^{-1}_{12\cdots n}(C)\equiv O^{-1}(C)\backslash H_{12\cdots n}. \tag{6}$$

If the set $H_{12\cdots n}$ is small enough, i.e., if $\epsilon\ll 1$, Eq. (5) can be used to obtain

$$\frac{1}{\tau^{(n)}_{12\cdots n}}\simeq\mu^{(n)}_{C12\cdots n}(H_{12\cdots n}). \tag{7}$$

Therefore, the lifetime $\tau^{(n)}_{12\cdots n}$ is approximately equal to the inverse of the c measure $\mu^{(n)}_{C12\cdots n}$ contained within the set $H_{12\cdots n}$. In the following sections, the c measure will be utilized as a tool for the theoretical description of the observed phenomena. From that perspective, Eq. (7) is of key importance for the theoretical analysis.

The measure $\mu^{(n)}_{C12\cdots n}$ is associated with the set $H_{12\cdots n}$. If we add one more hole, H_{n+1}, to the set $H_{12\cdots n}$, we obtain the set $H_{12\cdots nn+1}\equiv H_{12\cdots n}\cup H_{n+1}$, which defines the lifetime $\tau^{(n+1)}_{12\cdots nn+1}$ and the measure $\mu^{(n+1)}_{C12\cdots nn+1}$. Let $P_\epsilon\subset D$ denote an m-dimensional ball of radius ϵ (the same radius as the hole) within the phase space. For the theoretical treatment of the problem it is important to find the dependence of

$$\delta_{12\cdots n,n+1}(P_\epsilon)\equiv\mu^{(n+1)}_{C12\cdots nn+1}(P_\epsilon)-\mu^{(n)}_{C12\cdots n}(P_\epsilon) \tag{8}$$

on the position of the set P_ϵ on the attractor. The indices in $\delta_{12\cdots n,n+1}$ denote the indices of the set $H_{12\cdots n}$ and of the added hole H_{n+1}.

At first, we must introduce one definition. Consider two subsets of the phase space, $P,P'\subset D$. Suppose that we iterate the set P by using the modified map $O_{12\cdots n}$. Then, consider the images of the set P: $O^1_{12\cdots n}(P)$, $O^2_{12\cdots n}(P)$, . . . , $O^l_{12\cdots n}(P)$, ... Let

$$l^{(n)}_{12\cdots n}(P,P') \tag{9}$$

be the smallest positive integer l for which the section $O^l_{12\cdots n}(P)\cap P'\neq\emptyset$. Given a map O, this integer depends on the sets $H_{12\cdots n}$, P, and P'.

The quantity $\delta_{12\cdots n,n+1}(P_\epsilon)$ [Eq. (8)] depends on $l'\equiv l^{(n)}_{12\cdots n}(H_{n+1},P_\epsilon)$ [in what follows, $l'\equiv l^{(n)}_{12\cdots n}(H_{n+1},P_\epsilon)$]. There are two possibilities: (i) If $l'>l_c$, where l_c denotes some critical value, then $\delta_{12\cdots n,n+1}(P_\epsilon)\simeq 0$. (ii) If $l'\leqslant l_c$, then $\delta_{12\cdots n,n+1}(P_\epsilon)$ is smaller than zero. It can be shown that

$$\begin{aligned}\delta_{12\cdots n,n+1}(P_\epsilon)&\simeq-\mu^{(n)}_{C12\cdots n}(O^{-l'}_{12\cdots n}(P_\epsilon)\cap H_{n+1})\\ &\sim-e^{-\lambda_1 l'},\end{aligned} \tag{10}$$

i.e., the difference between the two measures decreases exponentially fast with the increase of l' (see the Appendix).

The critical value, l_c, is a small positive integer that is determined by the positive Lyapunov exponent of the map O (denoted λ_1). In Ref. [7] we have defined l_c as the smallest positive integer for which $e^{-\lambda_1 l_c}<0.1$. For the maps that we utilize, $l_c\sim 4$. A theoretical explanation of the statements above can be deduced from Ref. [7] (see the Appendix).

As an illustration of the c measures, Fig. 2(a) displays $\mu^{(4)}_{C1234}$ and $\mu^{(5)}_{C12345}$ for the tent map with four and five holes. The positions of the first four holes are taken as $\xi_1=0.338$, $\xi_2=0.331$, $\xi_3=0.411$, and $\xi_4=0.220$. The position of the added hole is $\xi_5=0.676$. The cells are chosen to be of the same size as the holes. Therefore, every cell C can be regarded as a set P_ϵ. Figure 2(b) shows the difference between these two measures, $\delta_{1234,5}(C)=\mu^{(5)}_{C12345}(C)-\mu^{(4)}_{C1234}(C)$. As we can see, $\delta_{1234,5}(C)$ is significantly smaller than zero only if $l^{(4)}_{1234}(H_5,C)\leqslant l_c$, i.e., in those cells that overlap with one of a few successive images of the added hole H_5. (For the tent map, $l_c\sim 4$.)

Note that $\Sigma_C\delta_{12\cdots n,n+1}(C)=0$ because the measures $\mu^{(n)}_{C12\cdots n}$ and $\mu^{(n+1)}_{C12\cdots nn+1}$ are normalized. Since for $l'\leqslant l_c$ the quantity $\delta_{12\cdots n,n+1}(P_\epsilon)$ is significantly smaller than zero, for the positions of the set P_ϵ where $l'>l_c$ [$\delta_{12\cdots n,n+1}(P_\epsilon)\simeq 0$], $\delta_{12\cdots n,n+1}(P_\epsilon)$ is actually slightly larger than zero [see Fig. (2)].

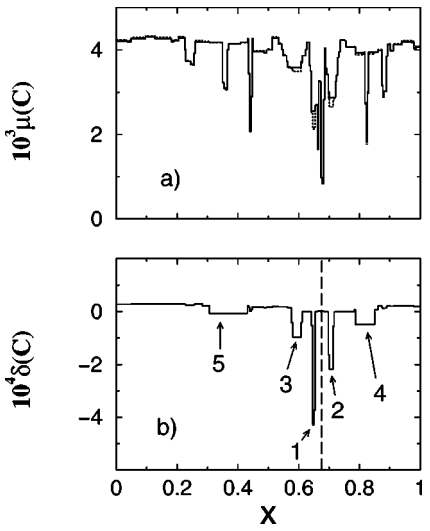

FIG. 2. (a) The c measures for the tent map with holes. The width of the holes is $2\epsilon=1/256$. The unit interval is divided into 256 cells (C) of equal size. The content of the c measures within a given cell C is drawn against the position of the cell (x). The measure $\mu^{(4)}_{C1234}$ ($\mu^{(5)}_{C12345}$) corresponding to four (five) holes is drawn with a solid (dotted) line. (b) The difference $\delta_{1234,5}(C)$ against the position of the cell. The position of the added hole H_5 is indicated with the vertical line. The positions of the first five images of H_5 are indicated with arrows.

In order to make the exposition clear, let us retrospect briefly on the notation. Given a map O, the choice of n holes defines the the lifetime $\tau^{(n)}_{12\cdots n}$, the auxiliary map $O_{12\cdots n}$, and the c measure $\mu^{(n)}_{C12\cdots n}$. For a given n, we can choose some smaller number of holes and define these quantities. For example, suppose that there are eight holes. We can choose three holes, say H_1, H_5, and H_7 that define $\tau^{(3)}_{157}$, O_{157}, and $\mu^{(3)}_{C157}$. As a similar example, $\delta_{17,5}(P_\epsilon)$ denotes $\mu^{(3)}_{C157}-\mu^{(2)}_{C17}$.

Furthermore, it is convenient to define

$$l_{P\to P'} \tag{11}$$

as the smallest positive integer l for which the section $O^l(P)\cap P'\neq\emptyset$. In simple words, the set P maps to the set P' in $l_{P\to P'}$ iterates. Given a map O, $l_{P\to P'}$ depends on the sets P and P'. From the definitions (11) and (9) it can be easily seen that $l_{P\to P'}\leqslant l^{(n)}_{12\cdots n}(P,P')$. Thus, if $l_{H_{n+1}\to P_\epsilon}>l_c$, then $\delta_{12\cdots n,n+1}(P_\epsilon)\simeq 0$.

III. THE TWO-HOLE LIFETIME AND THE PAIRWISE INTERACTION

In this section we study the lifetime $\tau^{(2)}_{12}$, which is defined as the average lifetime it takes for a randomly started trajectory to land in the set $H_1\cup H_2$ [see Eq. (2)]. The lifetime $\tau^{(2)}_{12}$ can be written in terms of the c measure [see Eq. (7)],

$$\frac{1}{\tau^{(2)}_{12}}=\mu^{(2)}_{C12}(H_1)+\mu^{(2)}_{C12}(H_2). \tag{12}$$

The comparison of the measures $\mu^{(n)}_{C12\cdots n}$ and $\mu^{(n+1)}_{C12\cdots nn+1}$ from the previous section leads us to investigate the substitutions $\mu^{(2)}_{C12}(H_1)\to\mu^{(1)}_{C1}(H_1)\simeq 1/\tau^{(1)}_1$ and $\mu^{(2)}_{C12}(H_2)\to\mu^{(1)}_{C2}(H_2)\simeq 1/\tau^{(1)}_2$. These substitutions lead to the following decomposition of the lifetime

$$\frac{1}{\tau^{(2)}_{12}}=\underbrace{\frac{1}{\tau^{(1)}_1}+\frac{1}{\tau^{(1)}_2}}_{\eta_1}+\underbrace{\Delta^{(2)}_{12}}_{\eta_2}. \tag{13}$$

The quantity $\Delta^{(2)}_{12}$, also referred to as the pairwise interaction between the holes H_1 and H_2, is defined by Eq. (13). From Eqs. (8), (12), and (13) it follows that

$$\Delta^{(2)}_{12}=\underbrace{\mu^{(2)}_{C12}(H_1)-\mu^{(1)}_{C1}(H_1)}_{\delta_{1,2}(H_1)}+\underbrace{\mu^{(2)}_{C12}(H_2)-\mu^{(1)}_{C2}(H_2)}_{\delta_{2,1}(H_2)}. \tag{14}$$

The functional dependence $\tau^{(2)}(\xi_1,\xi_2)$ is numerically and theoretically studied by investigating the functional dependencies $\tau^{(1)}(\xi_i)$ and $\Delta^{(2)}(\xi_1,\xi_2)$.

Let us consider results of a numerical experiment that is performed by using the tent map. The hole H_1 is located at the fixed position, $\xi_1=0.314\cdots$, on the attractor $A=[0,1]$. The position of the second hole, ξ_2, is moved across the attractor. The quantities $\tau^{(2)}_{12}$, η_1, and $\Delta^{(2)}_{12}$ are calculated. The size of both holes is constant, $2\epsilon=0.005$.

Figures 3(a), 3(b), and 3(c) display the average lifetime $\tau^{(2)}_{12}$, η_1^{-1}, and $\Delta^{(2)}_{12}$ as functions of the position of the moving hole H_2, respectively. We observe the following. (i) For most of the positions of the moving hole H_2, $\tau^{(2)}_{12}\simeq\eta_1^{-1}$, and $\Delta^{(2)}_{12}\simeq 0$. (ii) The quantity η_1^{-1} and hence $\tau^{(2)}_{12}$ are, on the average, approximately equal to $\mu_N(H_{12})^{-1}$. η_1^{-1} exhibits peak values only at the positions of short periodic orbits. Consequently, at these positions the lifetime $\tau^{(2)}_{12}$ obtains peak values as well. These peaks are labeled with asterisks in Figs. 3(a) and 3(b). (iii) When the moving hole H_2 overlaps with one of a few successive images (previous preimages) of the nonmoving hole H_1, then $\Delta^{(2)}_{12}$ obtains negative peak values. Consequently, $\tau^{(2)}_{12}$ exhibits a peak and becomes significantly larger than η_1^{-1}. These peaks are labeled with integer numbers. Positive (negative) integers denote $l_{H_1\to H_2}$ ($-l_{H_2\to H_1}$) [see quantity (11)]. For example, the peak labeled with 1 (-1) is located at the position of the first image (preimage) of the nonmoving hole H_1. (iv) The magnitude of the peaks labeled with $l_{H_1\to H_2}$ ($-l_{H_2\to H_1}$) decreases rapidly with the increase of $l_{H_1\to H_2}$ ($l_{H_2\to H_1}$).

Let us explain these observations.

(i) Since the holes H_1 and H_2 are very small, for most of the positions of the moving hole (H_2), the integers $l_{H_2\to H_1}$ and $l_{H_1\to H_2}$ will be larger than the critical value l_c. When $l_{H_2\to H_1}>l_c$ and $l_{H_1\to H_2}>l_c$, then $\delta_{1,2}(H_1)\simeq 0$ and

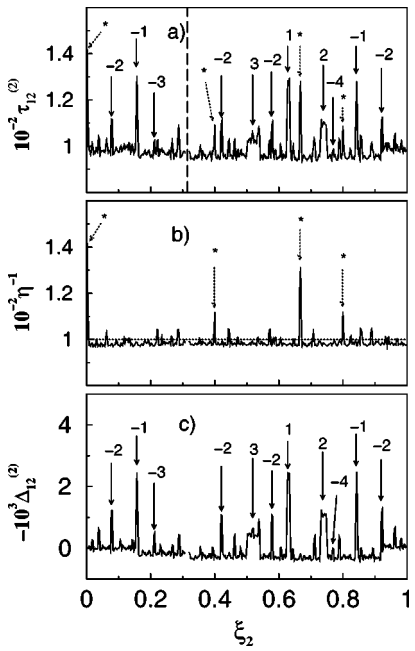

FIG. 3. Structure of the lifetime for the two-hole case. (a) The average lifetime $\tau_{12}^{(2)}$, (b) the approximation η^{-1} (solid line) and $\mu_N(H_{12})^{-1}$ (dotted line), and (c) the pairwise interaction $\Delta_{12}^{(2)}$ in dependence of the position of the moving hole H_2. The position of the nonmoving hole H_1 is indicated with the dashed vertical line.

$\delta_{2,1}(H_2)\simeq 0$, respectively [see quantity (8) and Eq. (14)]. This is equivalent to $\tau_{12}^{(2)}\simeq\eta_1^{-1}$ and $\Delta_{12}^{(2)}\simeq 0$.

(ii) Since η_1 is constructed solely from the one hole lifetimes, $\tau^{(1)}(\boldsymbol{\xi}_1)$ and $\tau^{(1)}(\boldsymbol{\xi}_2)$, the graph in Fig. 3(b) can be explained by using results from Ref. [7], where it has been demonstrated that for most of the positions $\boldsymbol{\xi}_i$, there is $\tau^{(1)}(\boldsymbol{\xi}_i)\simeq\mu_N(H_i)^{-1}$. We conclude that for most combinations of $\boldsymbol{\xi}_1$ and $\boldsymbol{\xi}_2$, the quantity η_1^{-1} and hence the lifetime $\tau_{12}^{(2)}$ are approximately equal to $[\mu_N(H_1)^{-1}+\mu_N(H_2)^{-1}]^{-1}=\mu_N(H_{12})^{-1}$. This conclusion is consistent with the previous reports [1,5,6,8,21].

For the tent map, the naturally invariant measure contained within a given interval on the attractor is equal to the length of that interval. Therefore, $\mu_N(H_2)=\mu_N(H_1)=2\epsilon=0.005$. This leads to ≈ 100 iterates as the average value of $\tau_{12}^{(2)}$ (see Fig. 3).

When the hole H_i encompasses a short periodic orbit, the lifetime $\tau^{(1)}(\boldsymbol{\xi}_i)$ is considerably longer than $\mu_N(H_i)^{-1}$ [7]. Consequently, when H_2 sweeps over a short periodic orbit, a peak is observed in both η_1^{-1} and $\tau_{12}^{(2)}$.

(iii) From results of the previous section [quantity (8)] and Eq. (14) it follows that when at least one of the integers $l_2^{(1)}(H_1,H_2)$ or $l_1^{(1)}(H_2,H_1)$ is smaller than l_c, then $\Delta_{12}^{(2)}$ is considerably smaller than zero. In our numerical experiment $l_{H_1\to H_2}=l_2^{(1)}(H_1,H_2)$ and $l_{H_2\to H_1}=l_1^{(1)}(H_2,H_1)$. Therefore, whenever $l_{H_1\to H_2}$ or $l_{H_2\to H_1}$ is smaller than the critical value l_c, a peak is observed in $\Delta_{12}^{(2)}$ and consequently in $\tau_{12}^{(2)}$.

(iv) In order to explain the magnitudes of these peaks, suppose that at least one of the integers $l_{H_1\to H_2}$ or $l_{H_2\to H_1}$ is smaller than l_c. Let us assume that $l_{H_2\to H_1}\leqslant l_c$ and $l_{H_1\to H_2}$

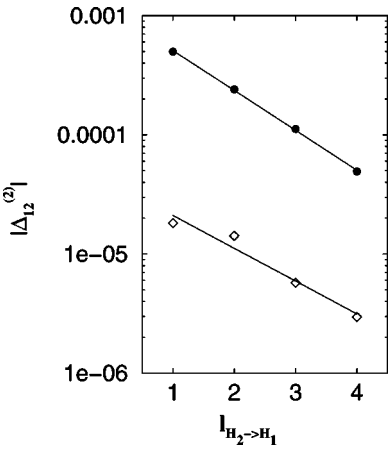

FIG. 4. The magnitude of the pairwise interaction $|\Delta_{12}^{(2)}|$ vs $l_{H_2\to H_1}$ ($l_{H_1\to H_2}>l_c$) for the tent (circles) and the Hénon map (diamonds). The size of the holes are $2\epsilon=0.001$ and $\epsilon=0.001$ for the tent and the Hénon map, respectively.

$>l_c$, i.e., the hole H_2 maps to the hole H_1 in just a few iterates. From Eqs. (10) and (14) it follows that

$$\Delta_{12}^{(2)}\simeq-\mu_{C1}^{(1)}(O_1^{-l_{H_2\to H_1}}(H_1)\cap H_2)\sim-e^{-\lambda_1 l_{H_2\to H_1}}, \tag{15}$$

i.e., the magnitude of the peak exhibited by $\Delta_{12}^{(2)}$ decreases exponentially fast with the increase of $l_{H_2\to H_1}$. Consequently, the peaks in $\tau_{12}^{(2)}$ labeled with negative (positive) integers decrease very rapidly with the increase of $l_{H_2\to H_1}$ ($l_{H_1\to H_2}$).

Note that the approximation $\mu_{C1}^{(1)}(O_1^{-l_{H_2\to H_1}}(H_1)\cap H_2)\sim e^{-\lambda_1 l_{H_2\to H_1}}$ assumes that the local stretching rates are approximately equal to the average stretching rate, described by the positive Lyapunov exponent (see the Appendix). For that reason, there may be some deviations from the exact exponential decrease. Furthermore, the slope of the $\ln|\Delta_{12}^{(2)}|$ vs $l_{H_2\to H_1}$ line can be larger or smaller than $-\lambda_1$, depending on the position of the holes, i.e., depending on the local stretching rates.

Figure 4 displays $|\Delta_{12}^{(2)}|$ vs $l_{H_2\to H_1}$ for the tent and the Hénon map (see Ref. [28] $a=1.4$, $b=0.3$). We see that the points are better correlated for the tent map than for the Hénon map. The aforementioned approximation [Eq. (15)] is exactly valid for the tent map: $|O'(x)|=2=e^{\lambda_1}$, $\forall x\in[0,1]$. The slopes of the lines are -0.77 and -0.6, while the ''theoretical'' values for the Lyapunov exponent are $\lambda_1=\ln 2=0.693\cdots$ and $\lambda_1=0.42$ [10] for the tent and the Hénon map, respectively.

Equation (15) can be interpreted in the following manner. If we associate the ''distance'' between the holes with the integers $l_{H_1\to H_2}$ and $l_{H_2\to H_1}$, then we can say that the pairwise interaction $\Delta_{12}^{(2)}$ decreases exponentially fast with the increase of ''distance.'' The exponential decrease is, on the average, determined by the positive Lyapunov exponent λ_1 of the map O. Therefore, λ_1 determines the ''effective range'' of the pairwise interaction. If the map is more cha-

otic, the ''range'' of the interaction is smaller, and for most of the positions of the holes $\Delta_{12}^{(2)} \simeq 0$.

When the positions of the holes are fixed, the pairwise interaction $\Delta_{12}^{(2)}$ obeys a power-law dependence on $\epsilon \ll 1$. This follows from the definition of $\Delta_{12}^{(2)}$ in Eq. (13), and the power-law dependence of the lifetimes on ϵ [1,6,8,13,21]. For ''almost every'' choice (with respect to the naturally invariant measure μ_N) of the positions $\boldsymbol{\xi}_i$ on the attractor, the lifetimes scale as $\tau_{12\cdots n}^{(n)} \sim \epsilon^{-D_1}$, where D_1 denotes the information dimension [1,6,8]. Consequently $\Delta_{12}^{(2)} \sim \epsilon^{D_1}$, i.e., $\Delta_{12}^{(2)}$ decreases with the decrease of ϵ. Therefore, the size of the holes ϵ can be thought of as the ''charge'' of the interaction.

The picture of a shadow as shown in Fig. 1(a) (shaded with diagonal lines), is suitable for 2D invertible maps, but not for 1D noninvertible maps. However, since $O^{-l}(H_j \cap O^l(H_i)) = O^{-l}(H_j) \cap H_i$, the hole H_j will be more intensively shadowed by the hole H_i if the intersection $O^{-l}(H_j) \cap H_i$ is larger, i.e., if the access $O^{-l}(H_j) \setminus H_i$ is smaller. This statement is applicable for both 1D noninvertible and 2D invertible maps. When the hole H_2 significantly shadows the hole H_1, i.e., when the intersection $O^{-l_{H_2 \to H_1}}(H_1) \cap H_2$ is large, the pairwise interaction $\Delta_{12}^{(2)}$ will exhibit a peak [see Eq. (15)]. Thus, the pairwise interaction $\Delta_{12}^{(2)}$ can be interpreted as the amount of shadowing between the holes.

From Eq. (15) it follows that the pairwise interaction and hence the lifetime exhibit a strong peak when $l_{H_1 \to H_2} = 1$ and $l_{H_2 \to H_1} = 1$, i.e., when the hole positions $\boldsymbol{\xi}_1$ and $\boldsymbol{\xi}_2$ lie on the points of an unstable periodic orbit of period two. For the tent map, when $\xi_1 = 0.4$, $\xi_2 = 0.8$, and $2\epsilon = 0.005$, then $\tau_{12}^{(2)} \simeq 193$ and $\Delta_{12}^{(2)} \simeq -2.53\ 10^{-3}$. By comparing these values with $\tau_{12}^{(2)}$ and $\Delta_{12}^{(2)}$ from Fig. 3, we see that this situation yields the most pronounced peak in both the lifetime and the pairwise interaction.

IV. THE THREE-HOLE LIFETIME AND THE RESIDUAL THREE-HOLE INTERACTION

In this section we study the lifetime $\tau_{123}^{(3)}$, defined as the average lifetime it takes for a randomly started trajectory to land in the set $H_1 \cup H_2 \cup H_3$. The functional dependence $\tau^{(3)}(\boldsymbol{\xi}_1, \boldsymbol{\xi}_2, \boldsymbol{\xi}_3)$ is studied through the following decomposition:

$$\frac{1}{\tau_{123}^{(3)}} = \underbrace{\frac{1}{\tau_1^{(1)}} + \frac{1}{\tau_2^{(1)}} + \frac{1}{\tau_3^{(1)}}}_{\eta_1} + \underbrace{\Delta_{12}^{(2)} + \Delta_{13}^{(2)} + \Delta_{23}^{(2)}}_{\eta_2} + \underbrace{\Delta_{123}^{(3)}}_{\eta_3}. \tag{16}$$

The justification for this decomposition will be clear after the numerical and theoretical analysis. The quantity $\Delta_{123}^{(3)}$ is referred to as the three-hole residual interaction. The functional dependencies $\tau^{(1)}(\boldsymbol{\xi}_i)$ and $\Delta^{(2)}(\boldsymbol{\xi}_i, \boldsymbol{\xi}_j)$, $i \neq j$, are well known from Ref. [7] and Sec. III of this manuscript, respectively. Hence, the only quantity that requires further analysis is the last term on the right-hand side of Eq. (16), i.e., the three-hole residual interaction.

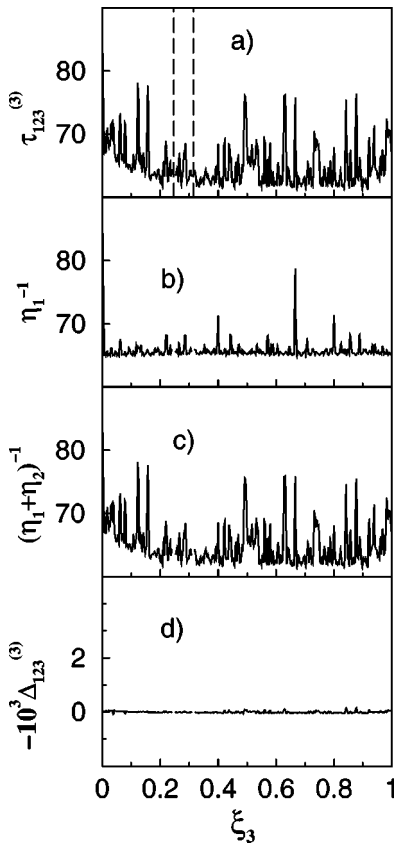

FIG. 5. The first numerical experiment: (a) The average lifetime $\tau_{123}^{(3)}$, (b) the approximation η_1^{-1}, (c) the approximation $(\eta_1 + \eta_2)^{-1}$, and (d) the residual three-hole interaction, $\Delta_{123}^{(3)}$, in dependence on the position of the moving hole H_3. The positions of the nonmoving holes, H_1 and H_2, are indicated with the vertical lines.

The lifetime $\tau_{123}^{(3)}$ is numerically studied by using the tent map. We have performed two numerical experiments. In both of them, the first and the second hole, H_1 and H_2, are located at fixed positions on the attractor [0,1]. The position of the third hole H_3 is changed across the attractor. All quantities from Eq. (16) are calculated. Parameters of the first numerical experiment are: the width of the holes $2\epsilon = 0.005$; and the positions of the nonmoving holes $\xi_1 = 0.314\cdots$ and $\xi_2 = 0.247$. The position of the hole H_1 is the same as in Fig. 3. From Fig. 3(c) it can be seen that in this first experiment, the pairwise interaction between the nonmoving holes is approximately zero, i.e., $\Delta_{12}^{(2)} \simeq 0$. Parameters of the second numerical experiment are $2\epsilon = 0.005$, $\xi_1 = 0.314\cdots$, and $\xi_2 = 0.157\cdots$. Note that only the position ξ_2 has changed. In the second numerical experiment, the pairwise interaction between the nonmoving holes is large, i.e., $\Delta_{12}^{(2)}$ has a peak. [In Fig. 3(c), this peak is positioned at $\xi_2 = 0.157\cdots$, and is labeled with -1.]

The results of the two experiments are displayed in Fig. 5 for the first, and in Fig. 6 for the second numerical experiment. The dependence of the lifetime $\tau_{123}^{(3)}$ on the position of

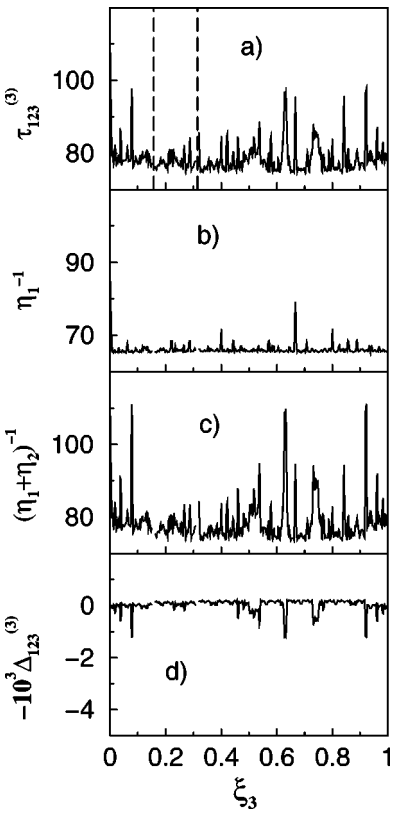

FIG. 6. The second numerical experiment: (a) The average lifetime $\tau^{(3)}_{123}$, (b) the approximation η_1^{-1}, (c) the approximation $(\eta_1+\eta_2)^{-1}$, and (d) $\Delta^{(3)}_{123}$ in dependence on the position of the moving hole H_3. The positions of the nonmoving holes are indicated with the vertical lines.

the moving hole H_3 is shown in Figs. 5(a) and 6(a) for the first and second numerical experiment, respectively. We observe similar patterns as in Fig. 3(a). The global behavior of the lifetime resembles the inverse of the naturally invariant measure contained within the set H_{123}, i.e., $\tau^{(3)}_{123} \sim \mu_N(H_{123})^{-1}$ [1,5,6,8,21]. The fact that $\tau^{(3)}_{123}$ is roughly a constant is a consequence of the features of the tent map (see Sec. III). At some positions of the moving hole we observe peaks in the lifetime. The peaks appear due to the shadowing effect. When H_3 sweeps over a short periodic orbit, then H_3 ''casts a shadow'' on itself and we observe a peak. When H_3 ''casts a shadow'' on one of the nonmoving holes, or when H_3 is shadowed by the nonmoving holes, then we also observe a peak.

In Figs. 5(b) and 6(b) we display the quantity η_1^{-1} [see Eq. (16)] for the first and second numerical experiment, respectively. The approximation $\tau^{(3)} \simeq \eta_1^{-1}$ does not include shadowing between different holes. In other words, it is applicable only when the pairwise interactions $\Delta^{(2)}_{ij}$ are insignificant. As we can see, the approximation η_1^{-1} is able to reproduce the global behavior of $\tau^{(3)}_{123}$ plus the peaks on the short periodic orbits. (This behavior of η_1^{-1} can be explained by using results from Ref. [7], see Sec. III.) Note that in the second experiment, the approximation η_1^{-1} is shifted downwards as compared to $\tau^{(3)}_{123}$. The cause of that lies in the fact that the non-moving holes, H_1 and H_2, significantly interact by the pairwise interaction $\Delta^{(2)}_{12}$. Therefore, for every position of the moving hole H_3, there is a systematic error in the approximation $\tau^{(3)} \simeq \eta_1^{-1}$.

However, when we include the pairwise interaction in the description of $\tau^{(3)}_{123}$, then we obtain a very good approximation. Figures 5(c) and 6(c) display the quantity $(\eta_1+\eta_2)^{-1}$ as a function of the moving hole [see Eq. (16)]. This approximation for $\tau^{(3)}_{123}$ includes the pairwise interactions. As we can see, in both Figs. 5(c) and 6(c) the quantity $(\eta_1+\eta_2)^{-1}$ describes the global behavior of the lifetime $\tau^{(3)}_{123}$ together with all of the peaks. (Note that in Fig. 6(c), $(\eta_1+\eta_2)^{-1}$ is not shifted downwards as compared to $\tau^{(3)}_{123}$ [Fig. 5(a)].) The functional dependence of the one-hole lifetimes and the pairwise interactions on the positions of the the holes is well known from the preceding section and Ref. [7]. Therefore, already at this point we understand almost all of the aspects of the functional dependence $\tau^{(3)}(\boldsymbol{\xi}_1, \boldsymbol{\xi}_2, \boldsymbol{\xi}_3)$.

It can be noticed that in the second experiment, the magnitude of the peaks is not well described by the approximation $(\eta_1+\eta_2)^{-1}$. In order to pictorially present this deviation, in Figs. 5(d) and 6(d) we display $\Delta^{(3)}_{123} = 1/\tau^{(3)}_{123} - (\eta_1+\eta_2)^{-1}$ for the first and the second experiment, respectively. In Fig. 5(d), $\Delta^{(3)}_{123} \approx 0$ for all of the positions of the moving hole H_3. However, in Fig. 6(d), $\Delta^{(3)}_{123}$ exhibits a peak for some positions of the moving hole. Inspection shows that the positions of these peaks coincide with the positions of the peaks exhibited by the pairwise interactions $\Delta^{(2)}_{13}$ and $\Delta^{(2)}_{23}$. Thus, the residual three-hole interaction exhibits a peak when all of the pairwise interactions $\Delta^{(2)}_{12}$, $\Delta^{(2)}_{13}$, and $\Delta^{(2)}_{23}$, are at their peak positions.

Let us explain the behavior of $\Delta^{(3)}_{123}$ theoretically. Imagine that one of the holes, e.g., H_2, is isolated from the other two, in the sense that the pairwise interactions $\Delta^{(2)}_{12} \simeq 0$ $(l_{H_1 \to H_2} > l_c, \quad l_{H_2 \to H_1} > l_c)$ and $\Delta^{(2)}_{23} \simeq 0$ $(l_{H_2 \to H_3} > l_c, \quad l_{H_3 \to H_2} > l_c)$. At this point, we are not interested in the strength of the pairwise interaction $\Delta^{(2)}_{13}$. The average lifetime $\tau^{(3)}_{123}$ can be written in terms of the c measure

$$\begin{aligned}
\frac{1}{\tau^{(3)}_{123}} &\simeq \mu^{(3)}_{C123}(H_1) + \mu^{(3)}_{C123}(H_2) + \mu^{(3)}_{C123}(H_3) \\
&\simeq \mu^{(2)}_{C13}(H_1) + \mu^{(1)}_{C2}(H_2) + \mu^{(2)}_{C13}(H_3) \\
&\simeq \frac{1}{\tau^{(2)}_{13}} + \frac{1}{\tau^{(1)}_{2}} \\
&\simeq \frac{1}{\tau^{(1)}_{1}} + \frac{1}{\tau^{(1)}_{2}} + \frac{1}{\tau^{(1)}_{3}} + \Delta^{(2)}_{13}. \qquad (17)
\end{aligned}$$

The approximations $\mu^{(3)}_{C123}(H_2) \simeq \mu^{(2)}_{C12}(H_2) \simeq \mu^{(1)}_{C2}(H_2)$ follow from $l_{H_3 \to H_2} > l_c$ and $l_{H_1 \to H_2} > l_c$, respectively. Similarly, the approximation $\mu^{(3)}_{C123}(H_1) \simeq \mu^{(2)}_{C13}(H_1)$ follows from $l_{H_2 \to H_1} > l_c$, and $\mu^{(3)}_{C123}(H_3) \simeq \mu^{(2)}_{C13}(H_3)$ follows from $l_{H_2 \to H_3} > l_c$. Since $\Delta^{(2)}_{12} \simeq 0$ and $\Delta^{(2)}_{23} \simeq 0$, from Eqs. (16) and

(17) we obtain $\Delta^{(3)}_{123} \simeq 0$. In the first experiment, for every position of the moving hole H_3, one of the holes is always isolated in the aforementioned sense. Therefore, the considerations above [Eq. (17)] theoretically explain the absence of the three-hole residual interaction in the first experiment [Fig. 5(d)].

Imagine the following situation, the holes H_1 and H_3 significantly interact by the pairwise interaction $\Delta^{(2)}_{13}$. To be more specific, assume that $l_{H_3 \to H_1} \leqslant l_c$ and $l_{H_1 \to H_3} > l_c$. Assume that we position the hole H_2 ''in between'' the holes H_3 and H_1, in the sense that $O^{l_{H_3 \to H_2}}(\boldsymbol{\xi}_3) = \boldsymbol{\xi}_2$, $O^{l_{H_2 \to H_1}}(\boldsymbol{\xi}_2) = \boldsymbol{\xi}_1$, $l_{H_3 \to H_1} = l_{H_3 \to H_2} + l_{H_2 \to H_1}$. Evidently, $\Delta^{(2)}_{23}$ and $\Delta^{(2)}_{12}$ are significant as well. For simplicity, we assume that $l_{H_1 \to H_2} > l_c$ and $l_{H_2 \to H_3} > l_c$. This kind of situation creates peaks shown in Fig. 6(d). From Eqs. (7) and (16) it follows that

$$\Delta^{(3)}_{123} \simeq \delta_{23,1}(H_3) - \delta_{3,1}(H_3) + \delta_{23,1}(H_2) - \delta_{2,1}(H_2) + \delta_{12,3}(H_1) - \delta_{1,3}(H_1). \tag{18}$$

The first two terms in Eq. (18) are ≈ 0 because $l_{H_1 \to H_3} > l_c$. Since $l_{H_1 \to H_2} > l_c$, the third and the fourth term are ≈ 0. The fifth term depends on $l^{(2)}_{12}(H_3, H_1)$, while the sixth term depends on $l^{(1)}_{1}(H_3, H_1)$. Since H_2 is ''in the middle'' of H_3 and H_1, $l^{(2)}_{12}(H_3, H_1) > l_{H_3 \to H_1}$, and most likely $l^{(2)}_{12}(H_3, H_1) > l_c$. This leads to $\delta_{12,3}(H_1) \simeq 0$. Since $l_{H_1 \to H_3} > l_c$ and $l^{(1)}_{1}(H_3, H_1) = l_{H_3 \to H_1} \leqslant l_c$, the sixth term is $\delta_{1,3}(H_1) \simeq \Delta^{(2)}_{13}$. Thus, for this particular situation of the positions of the holes, the magnitude of the residual three-hole interaction is $\Delta^{(3)}_{123} \simeq -\Delta^{(2)}_{13}$.

Let us explain this result in simple words. The approximation $\tau^{(3)}_{123} \simeq \eta_1^{-1}$ is applicable only when there is no shadowing between different holes. If some shadowing exists, η_1^{-1} is an underestimate because shadowing prolongs the lifetime. The total amount of shadowing is given by the difference $1/\tau^{(3)}_{123} - \eta_1$. It seems reasonable that the total amount of shadowing can be represented by the sum over all pairwise interactions, i.e., $1/\tau^{(3)}_{123} - \eta_1 \simeq \Delta^{(2)}_{12} + \Delta^{(2)}_{13} + \Delta^{(2)}_{23}$. However, the pairwise interaction between two holes, as defined by Eq. (13), does not depend on the position of the third hole. Thus, when H_2 is ''in between'' the holes H_3 and H_1, i.e., when $O^{l_{H_3 \to H_2}}(\boldsymbol{\xi}_3) = \boldsymbol{\xi}_2$, $O^{l_{H_2 \to H_1}}(\boldsymbol{\xi}_2) = \boldsymbol{\xi}_1$, $l_{H_3 \to H_1} = l_{H_3 \to H_2} + l_{H_2 \to H_1} \leqslant l_c$, then the hole H_2 prevents H_3 from casting a shadow on the hole H_1 (as an eclipse). For that reason, $\Delta^{(2)}_{12} + \Delta^{(2)}_{13} + \Delta^{(2)}_{23}$ is larger than the total amount of shadowing by approximately $\Delta^{(2)}_{13}$, i.e., $\Delta^{(3)}_{123} \simeq -\Delta^{(2)}_{13}$. (Since the peaks in the pairwise interactions are negative, the peaks in the residual three-hole interactions are positive.)

The residual three-hole interaction $\Delta^{(3)}_{123}$ can exhibit a peak for some other arrangement of the hole positions. For example, when the holes are on a periodic orbit of period 3 we also observe a peak in $\Delta^{(3)}_{123}$. For the tent map, when $\xi_1 = 2/7$, $\xi_2 = 4/7$, $\xi_3 = 6/7$, and $2\epsilon = 0.005$, then $\tau^{(3)}_{123} \simeq 127$ and $\Delta^{(3)}_{123} \simeq 1.86 \times 10^{-3}$. By comparing these values with $\tau^{(3)}_{123}$ and $\Delta^{(3)}_{123}$ from Figs. 5(a), 6(a), and 6(d), we see that this situation yields the most pronounced peak in both the lifetime and the three-hole residual interaction. These other cases can be theoretically treated by using the same strategy as in Eq. (18).

We have seen that the presence of the third hole can prevent shadowing between the other two holes. For this reason, we have two alternative approaches to describing the lifetime $\tau^{(3)}_{123}$. (i) When the third hole is introduced, we can redefine the pairwise interactions in order to write $1/\tau^{(3)}_{123}$ as a sum of one hole escape rates, $\Sigma^{(3)}_{i=1} 1/\tau^{(1)}_i$, plus the new, redefined pairwise interactions. These new pairwise interactions would have to depend on the positions of all holes involved. (ii) The second approach is to simply write the total amount of shadowing as a sum of the old pairwise interactions [defined by Eq. (13)] plus the residual three-hole interaction. We have chosen the latter approach. From Eq. (17) it follows that $\Delta^{(3)}_{123}$ can exhibit a peak value only if all of the three holes are mutually involved in the shadowing interactions.

V. GENERALIZATION

In the preceding two sections, we have investigated the lifetimes $\tau^{(2)}$ and $\tau^{(3)}$. An inductive approach leads to the study of the n-hole lifetime $\tau^{(n)}$ for $n \geqslant 4$. Suppose that we have studied the lifetimes $\tau^{(4)}$, $\tau^{(5)}$, ..., $\tau^{(n-1)}$, and the corresponding residual many-hole interactions, $\Delta^{(4)}$, $\Delta^{(5)}$, ..., $\Delta^{(n-1)}$, respectively. In this section we will study the following decomposition:

$$\frac{1}{\tau^{(n)}_{12\cdots n}} = \sum_{k=1}^{n} \eta_k, \tag{19}$$

where

$$\eta_1 = \sum_{i_1=1}^{n} \frac{1}{\tau^{(1)}_{i_1}}, \tag{20}$$

and

$$\eta_k = \sum_{i_1=1}^{n-k+1} \sum_{i_2=i_1+1}^{n-k+2} \cdots \sum_{i_k=i_{k-1}+1}^{n} \Delta^{(k)}_{i_1 i_2 i_3 \cdots i_k}, \quad k \geqslant 2. \tag{21}$$

Equations (13) and (16) are special cases of Eq. (19) for $n = 2$ and $n = 3$, respectively. From Eq. (21) it follows that the kth contribution to the lifetime, η_k, is the sum of $\binom{n}{k}$ residual k-hole interactions [$\Delta^{(k)}$]. Equations (19), (20), and (21) define the residual n-hole interaction $\Delta^{(n)}_{12\cdots n}$.

The escape rate $1/\tau^{(n)}_{12\cdots n}$ is in the first approximation given by the one-hole escape rates $1/\tau^{(n)}_{12\cdots n} \simeq \eta_1$ [see Eq. (20)]. This approximation is applicable only when there is no shadowing. The total amount of shadowing is $\Sigma^{n}_{k=2} \eta_k$. From Eqs. (19) and (21) it follows that the total amount of shadowing has complicated structure. By assuming that we know the behavior of $\Delta^{(k)}$ for $k < n$, the most interesting term in decomposition (19) is the residual n-hole interaction $\Delta^{(n)}_{12\cdots n}$.

From the behavior of $\Delta^{(3)}_{123}$ we conjecture that $\Delta^{(n)}_{12\cdots n}$ obtains a peak value only if all n holes are mutually involved in the shadowing interactions. The most obvious physical realization for this to occur is when the positions $\boldsymbol{\xi}_i$, $i=1,2,\ldots,n$, coincide with the points of an unstable periodic orbit of period n [see Eq. (3)]. In this case that is of particular interest to the field of controlling chaos, every hole strongly shadows the next one, i.e., H_1 shadows H_2, H_2 shadows H_3, etc. [see Fig. 1(b)].

This specific arrangement can be theoretically treated by utilizing the c measure. We have analytically derived the contribution of $\Delta^{(n)}_{12\cdots n}$ within decomposition (19), i.e., $|\Delta^{(n)}_{12\cdots n}|/[\tau^{(n)}_{12\cdots n}]^{-1}$ as a function of n for $n=2$, 3, and 4. From these derivations a conjecture follows that

$$\frac{|\Delta^{(n)}_{12\cdots n}|}{[\tau^{(n)}_{12\cdots n}]^{-1}} \sim e^{-\lambda_1(n-1)}. \tag{22}$$

The approximation that leads to Eq. (22) is a bit rough. Let $\Lambda_{\mathrm{unst},i}$, $i=1,2,\ldots,n$ denote $|O'(\xi_i)|$ for 1D maps. For 2D maps, let $\Lambda_{\mathrm{unst},i}$ denote the magnitude of the eigenvalue of $DO(\boldsymbol{\xi}_i)$ that corresponds to the unstable direction (O is a 2D map). $DO(\boldsymbol{\xi}_i)$ denotes the Jacobian matrix of partial derivatives calculated at $\boldsymbol{\xi}_i$. The approximation is $\Lambda_{\mathrm{unst},i} \simeq \exp \lambda_1$, $i=1,2,\ldots,n$.

In order to test conjecture (22), within the attractors of the tent map, generalized Baker map (see Ref. [6], p. 75, $\lambda_a=0.35$, $\lambda_b=0.40$, $\alpha=0.40$, $\beta=0.60$), and the Hénon map [28], we find some periodic orbits of prime period 2,3, . . . ,10, provided they exist. Then we center n holes on the points of the unstable periodic orbit of period n and calculate $|\Delta^{(n)}_{12\cdots n}|/[\tau^{(n)}_{12\cdots n}]^{-1}$. Figure 7 displays $|\Delta^{(n)}_{12\cdots n}|/[\tau^{(n)}_{12\cdots n}]^{-1}$ against n. For the tent map, the Baker map, and the Hénon map, the slope of the $\ln|\Delta^{(n)}_{12\cdots n}|/[\tau^{(n)}_{12\cdots n}]^{-1}$ vs n graph obtained from the numerical data is -0.700, -0.60, and -0.49, respectively. The ''theoretical'' value of λ_1 for these maps is $\ln 2=0.693\cdots$, 0.636, and 0.42 [10], respectively. The points on the graphs are far better correlated for the tent map than for the other two maps. This is due to the fact that the approximation above is exactly valid for the tent map, i.e., $|O'(x)|=\exp(\ln 2)$, $\forall x \in [0,1]$. Equation (22) strongly underpins the idea that λ_1 determines the ''effective range'' of the shadowing interaction.

In addition to the numerical experiment presented above, it is interesting to examine the total contribution of the residual k-hole interactions, i.e., $\eta_k/[\tau^{(n)}_{12\cdots n}]^{-1}$, within the sum in Eq. (19). We perform two numerical experiments by using the tent map. In the first one, we randomly choose 100 arrangements of the hole positions $(\xi_1,\xi_2,\ldots,\xi_n)$. For every random choice, the contributions $\eta_k/[\tau^{(n)}_{12\cdots n}]^{-1}$ are calculated. Then we calculate the average value of the kth contribution, i.e., $\langle \eta_k/[\tau^{(n)}_{12\cdots n}]^{-1}\rangle$. In the second experiment, we position ten holes at the points of an unstable periodic orbit of period 10. Then we calculate the kth contribution $\eta_k/[\tau^{(n)}_{12\cdots n}]^{-1}$, for $k=1,2,\ldots,10$. Figure 8 displays

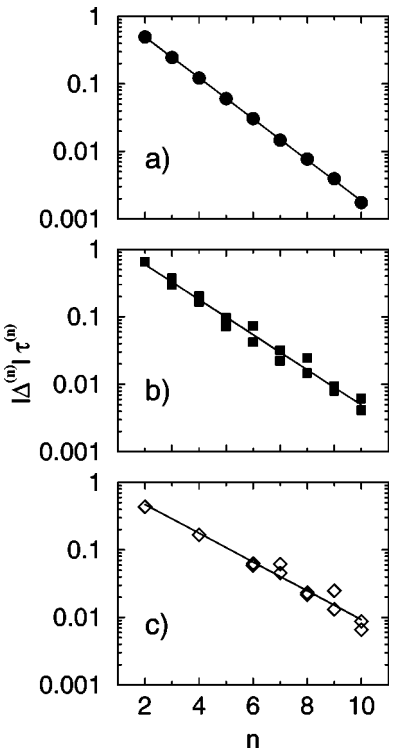

FIG. 7. $|\Delta^{(n)}_{12\cdots n}|/[\tau^{(n)}_{12\cdots n}]^{-1}$ vs n. The contribution of the n-hole residual interaction, within decomposition (19), decreases exponentially fast with the increase of n. The holes H_i are located on n points of an unstable periodic orbit of period n. $|\Delta^{(n)}_{12\cdots n}|/[\tau^{(n)}_{12\cdots n}]^{-1}$ for (a) the tent map, $2\epsilon=9.77\cdots10^{-4}$, (b) the Baker map, $\epsilon=0.005$, and (c) the Hénon map, $\epsilon=0.001$. See text for further details.

$\langle \eta_k/[\tau^{(n)}_{12\cdots n}]^{-1}\rangle$ and $\eta_k/[\tau^{(n)}_{12\cdots n}]^{-1}$ vs k for the first and the second experiment, respectively.

From the first numerical experiment, we see that the contributions $\eta_k/[\tau^{(n)}_{12\cdots n}]^{-1}$ decrease very rapidly with the increase of k. In order to understand this behavior, consider $\Delta^{(k)}_{i_1 i_2 i_3 \cdots i_k}$ corresponding to a random choice of k hole posi-

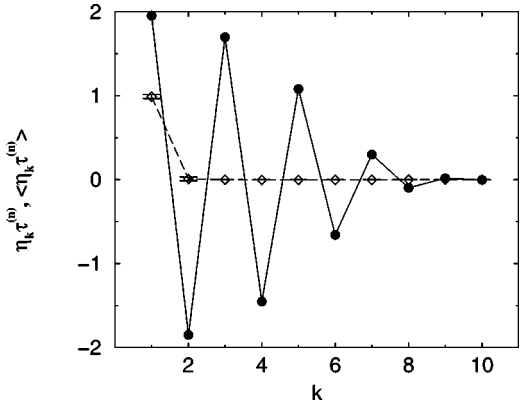

FIG. 8. The contribution $\eta_k/[\tau^{(n)}_{12\cdots n}]^{-1}$ vs k for the holes located on an unstable periodic orbit (closed circles). The average value $\langle \eta_k/[\tau^{(n)}_{12\cdots n}]^{-1}\rangle$ vs k for 100 randomly chosen positions $(\xi_1,\xi_2,\ldots,\xi_n)$ (open diamonds). The r.m.s. deviation of $\langle \eta_k/[\tau^{(n)}_{12\cdots n}]^{-1}\rangle$ (horizontal error bars). $2\epsilon=9.77\cdots10^{-4}$.

tions $\boldsymbol{\xi}_{i_1}$, $\boldsymbol{\xi}_{i_2}$, ..., $\boldsymbol{\xi}_{i_k}$. For some random choice of the hole positions, it is highly unlikely that all of these k holes would be mutually involved in the shadowing interactions (e.g., that they are on a periodic orbit of period k). In other words, it is most likely that $\Delta^{(k)}_{i_1 i_2 i_3 \cdots i_k} \simeq 0$.

Results of the second numerical experiment are strongly distinguished from results of the first numerical experiment. We see that the contributions η_k do not decrease rapidly at all. The sign of η_k is positive (negative) for odd (even) values of k. This follows from the definition of the many-hole interactions. We have seen that $\Delta^{(2)}$ obtains negative peaks [see Eq. (15)]. Study of Eq. (18) shows that $\Delta^{(3)}$ exhibits a peak when the sum over pairwise interactions becomes an overestimate for the total amount of shadowing. Thus, since the pairwise interactions are negative, $\Delta^{(3)}$ exhibits positive peaks. This behavior is inductively reflected into the k-hole residual interactions and consequently into the contributions η_k.

We conclude that both the residual n-hole interaction and the lifetime $\tau^{(n)}_{12\cdots n}$ distinguish itself when the holes are located on an unstable periodic orbit of period n, i.e., in the case of interest to the field of controlling chaos. This is a consequence of strong shadowing.

VI. THE CORRELATION BETWEEN THE AVERAGE LIFETIME AND THE VISITATION FREQUENCY

It is clear that if a certain region on a chaotic attractor is visited more frequently by typical trajectories, the average lifetime it takes for an orbit to land in that region will be smaller. Therefore, $\mu_N(H_{12\cdots n})^{-1}$ [$\mu_N \equiv$ the naturally invariant measure] may be used as an estimate for the average lifetime $\tau^{(n)}_{12\cdots n}$.

Let us consider the lifetime $\tau^{(2)}_{ij}$ corresponding to the situation that is displayed in Fig. 1(a). Although a trajectory cannot land (for the first time) within the set H_{ij} by landing within the shadow $O^l(H_i) \cap H_j$, the estimate for the lifetime $\tau^{(2)}_{ij}$ given by $\mu_N(H_{ij})^{-1}$ includes the visitation frequency by typical trajectories to the shadowed region.

We conclude that the estimate $\mu_N(H_{12\cdots n})^{-1}$ for the lifetime $\tau^{(n)}_{12\cdots n}$ does not include the shadowing effect. When the holes are located at n points of an unstable periodic orbit, then the shadowing is extremely large. Since shadowing prolongs the lifetime, the estimate given by $\mu_N(H_{12\cdots n})^{-1}$ can be significantly smaller than the average lifetime $\tau^{(n)}_{12\cdots n}$.

In Ref. [7] we have studied the average lifetime $\tau^{(1)}(\boldsymbol{\xi}_1)$ corresponding to just one hole (e.g., H_1). It has been demonstrated that the ratio $\tau^{(1)}(\boldsymbol{\xi}_1)/\mu_N(H_1)^{-1}$ depends on the magnitude of the expanding eigenvalue (call it Λ_u) of the shortest periodic orbit within the hole H_1 [7]:

$$\tau^{(1)}(\boldsymbol{\xi}_1) \simeq \frac{1}{1-\Lambda_u^{-1}} \mu_N(H_1)^{-1}. \tag{23}$$

Here we generalize this result to the n-hole case.

In this section we assume that the positions of the holes ($\boldsymbol{\xi}_i$) coincide with points of an unstable periodic orbit of period n [see Eq. (3)]. As we have already said, this situation is of interest to the field of controlling chaos.

From Eqs. (7) and (5) it follows that

$$\frac{1}{\tau^{(n)}_{12\cdots n}} \simeq \sum_{i=1}^{n} \mu^{(n)}_{C12\cdots n}(H_i) \simeq \sum_{i=1}^{n} \mu^{(n)}_{C12\cdots n}(O^{-1}(H_{i+1}) \setminus H_i). \tag{24}$$

The measure μ_N is invariant, i.e., $\mu_N(P) = \mu_N(O^{-1}(P))$, where $P \subset D$. From this, we can write

$$\mu_N(H_{12\cdots n}) = \sum_{i=1}^{n} \{\mu_N(O^{-1}(H_{i+1}) \cap H_i) + \mu_N(O^{-1}(H_{i+1}) \setminus H_i)\}. \tag{25}$$

In Eqs. (24) and (25) $H_{n+1} \equiv H_1$. This notation is kept throughout this section.

In Ref. [7] we have compared the c measure corresponding to just one hole $\mu^{(1)}_{C1}$, with the naturally invariant measure μ_N. Recalling the definition of P_ϵ, in Ref. [7] it has been shown that if $l_{H_1 \to P_\epsilon} > l_c$, then $\mu_{C1}(P_\epsilon) \simeq \mu_N(P_\epsilon)$. Otherwise, $\mu_{C1}(P_\epsilon)$ is significantly smaller than $\mu_N(P_\epsilon)$. In simple words, a significant difference between $\mu_N(P_\epsilon)$ and $\mu_{C1}(P_\epsilon)$ can occur only if P_ϵ overlaps with one of a few successive images of H_1: $O^1(H_1)$, $O^2(H_1)$, ..., $O^{l_c}(H_1)$.

Let us make a projection of that result to obtain the relation between Eqs. (24) and (25). Since the holes are located on an unstable periodic orbit, the sets $O^1(H_i)$, $O^2(H_i)$, ..., $O^{l_c}(H_i)$, are ellipsoidal regions centered at the points $\boldsymbol{\xi}_{i+1}$, $\boldsymbol{\xi}_{i+2}$, ..., $\boldsymbol{\xi}_{i+l_c}$, respectively. These ellipsoidal regions are stretched along the unstable manifolds. The difference between $\mu^{(n)}_{C12\cdots n}(P_\epsilon)$ and $\mu_N(P_\epsilon)$ can be considerable only if P_ϵ overlaps with one of these ellipsoidal regions. Since the sets $O^{-1}(H_{i+1}) \setminus H_i$, $i = 1,2,\ldots,n$, are stretched along the stable manifolds, and since they do not overlap with the aforementioned ellipsoidal regions, we approximately write

$$\mu^{(n)}_{C12\cdots n}(O^{-1}(H_{i+1}) \setminus H_i) \simeq \mu_N(O^{-1}(H_{i+1}) \setminus H_i), \tag{26}$$

where $i = 1,2,\ldots,n$. [Equation (26) can be justified for 1D maps by similar arguments.] This leads us to the relation between the lifetime $\tau^{(n)}_{12\cdots n}$ and the visitation frequences $\mu_N(H_i)$, $i = 1,2,\ldots,n$:

$$\frac{1}{\tau^{(n)}_{12\ldots n}} \simeq \sum_{i=1}^{n} \mu_N(O^{-1}(H_{i+1}) \setminus H_i) = \sum_{i=1}^{n} \mu_N(H_i) \left(1 - \frac{\mu_N(O^{-1}(H_{i+1}) \cap H_i)}{\mu_N(H_i)}\right). \tag{27}$$

Equation (27) can be applied for holes of different shapes as long as they are sufficiently small. If (for 2D maps) we tailor the holes as rectangles with sides of length 2ϵ parallel to the stable and unstable manifold segments, and if we assume

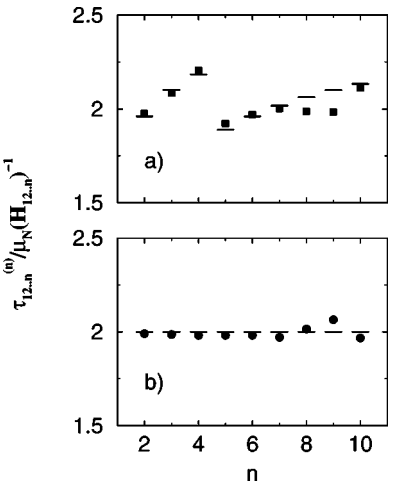

FIG. 9. Numerically evaluated ratio $\tau^{(n)}_{12\cdots n}/\mu_N(H_{12\cdots n})^{-1}$ for (a) the Baker map (closed squares), and (b) the tent map (closed circles) in comparison to $(1-\Lambda_u^{-1/n})^{-1}$ (horizontal bars). n holes are centered on the points of an unstable periodic orbit of period n. The size of the holes is $\epsilon=0.005$ and $2\epsilon=0.000488\cdots$ for the Baker and the tent map, respectively.

that the naturally invariant measure is smooth along the unstable directions [10], then we can write

$$\frac{\mu_N(O^{-1}(H_{i+1})\cap H_i)}{\mu_N(H_i)}\simeq\Lambda_{\mathrm{unst},i}, \quad i=1,2,\ldots,n. \quad (28)$$

From Eqs. (27) and (28) we obtain

$$\frac{1}{\tau^{(n)}_{12\cdots n}}\simeq\sum_{i=1}^{n}\mu_N(H_i)(1-\Lambda^{-1}_{\mathrm{unst},i}). \quad (29)$$

Equation (29) can be further simplified. Let Λ_u denote the magnitude of the unstable eigenvalue of the unstable periodic orbit, i.e., $\Lambda_u=\Pi_{i=1}^{n}\Lambda_{\mathrm{unst},i}$. If we approximate that $\Lambda_{\mathrm{unst},i}\simeq\Lambda_u^{1/n}$, for $i=1,2,\ldots,n$, then Eq. (29) transforms into

$$\tau^{(n)}_{12\cdots n}\simeq\frac{1}{1-\Lambda_u^{-1/n}}\mu_N(H_{12\cdots n})^{-1}. \quad (30)$$

Equation (30) is the generalization of Eq. (23) for the case when n holes are positioned on an unstable periodic orbit of period n. The utility value of Eq. (23) and consequently Eq. (30) for applications has been discussed in Ref. [7].

In Fig. 9 we display a test of Eq. (30) on the Baker and the tent map. As we can see, the derived formula [Eq. (30)] is a good approximation. For some unstable periodic orbits, the local stretching rates at different points of the unstable periodic orbit may be considerably different, i.e., the approximation $\Lambda_{\mathrm{unst},i}\simeq\Lambda_u^{1/n}$ may be not applicable. For these unstable periodic orbits, it is better to use more robust approximations such as Eqs. (27) or (29).

VII. CONCLUSION

In conclusion, we have studied the average lifetime $\tau^{(n)}_{12\cdots n}$ it takes for a randomly initiated trajectory to land within the set of n holes, $H_{12\cdots n}$, on the chaotic attractor of the map O. We have demonstrated that $\tau^{(n)}_{12\cdots n}$ exhibits very sensitive dependence on the positions of the holes. For some positions of the holes, $\tau^{(n)}_{12\cdots n}$ exhibits sharp peaks. These peaks originate from the shadowing effect. The amount of shadowing between the holes and hence the strength of the peaks in the lifetime has been quantitatively described in terms of the many-hole interactions.

The construction and the analysis of the many-hole interactions are the main result of this paper. We have demonstrated that these interactions have very short ''effective range.'' The ''effective range'' of the many-hole interactions has been associated with the positive Lyapunov exponent of the map O.

We have demonstrated that when the holes are located on the points of an unstable periodic orbit of period n, the amount of shadowing is very large. Consequently, the average lifetime exhibits one of its most pronounced peak values, and becomes considerably prolonged as compared to the inverse of the naturally invariant measure contained within the set $H_{12\cdots n}$. The formula [Eq. (30)] that describes this discrepancy has been derived and tested on some paradigmatic maps.

APPENDIX

In Ref. [7] the naturally invariant measure (μ_N) of the map O has been theoretically compared with the c measure corresponding to just one hole (say $\mu^{(1)}_{C1}$). It has been demonstrated that the ratio $\mu^{(1)}_{C1}(P_\epsilon)/\mu_N(P_\epsilon)$ depends on the integer $l_{H_1\to P_\epsilon}$. Moreover, this ratio was shown to be considerably smaller than 1 only for very small values of $l_{H_1\to P_\epsilon}$.

In this appendix we will extend this result to find the behavior of the quantity $\delta_{12\cdots n,n+1}(P_\epsilon)$ in dependence of the integer $l^{(n)}_{12\cdots n}(H_{n+1},P_\epsilon)$. The size of the first n holes, H_1, H_2, . . . , and H_n is denoted with $\epsilon\ll 1$ as in the rest of the manuscript. However, the added hole H_{n+1} is to be distinguished from other holes. Therefore, its size is denoted with ϵ_{n+1}.

Imagine that we cover the chaotic attractor with cells (call them $C\subset D$) from a very fine grid. For 1D (2D) maps, we choose cells to be intervals (squares) of length (area) 2ϵ $(4\epsilon^2)$, i.e., the cells are of the same size as the holes H_i.

Now we argue heuristically that if $\epsilon\ll 1$, then $\mu^{(n)}_{C12\cdots n}(C)\simeq\mu^{(n+1)}_{C12\cdots nn+1}(C)$ in most of the cells C, i.e., the two measures appear globally identical (see Fig. 2). A set of points on the attractor that never visits the set $H_{12\cdots n}$ $(H_{12\cdots nn+1})$ under the dynamics of the map O is an embedded chaotic repeller [18,19,25]. Let us denote this set with $\Lambda^{(n)}_{12\cdots n}$ $(\Lambda^{(n+1)}_{12\cdots nn+1})$. It is evident that $\Lambda^{(n+1)}_{12\cdots nn+1}\subset\Lambda^{(n)}_{12\cdots n}$. As ϵ_{n+1} decreases to zero the repeller $\Lambda^{(n+1)}_{12\cdots nn+1}$ gradually becomes identical to $\Lambda^{(n)}_{12\cdots n}$.

The measure $\mu^{(n)}_{C12\cdots n}$ $(\mu^{(n+1)}_{C12\cdots nn+1})$ is concentrated along the unstable directions from the repeller

$\Lambda^{(n)}_{12\cdots n}$ ($\Lambda^{(n+1)}_{12\cdots nn+1}$) up to the set $H_{12\cdots n}$ ($H_{12\cdots nn+1}$) [13–15,17–20]. Thus, as ϵ_{n+1} decreases to zero, the measure $\mu^{(n+1)}_{C12\cdots nn+1}$ gradually becomes identical to $\mu^{(n)}_{C12\cdots n}$. (Finally, for $\epsilon_{n+1}=0$, $\mu^{(n+1)}_{C12\cdots nn+1}\equiv\mu^{(n)}_{C12\cdots n}$.) Therefore, if ϵ_{n+1} is sufficiently small, then $\mu^{(n)}_{C12\cdots n}(C)\simeq\mu^{(n+1)}_{C12\cdots nn+1}(C)$ in most of the cells C. Since $\epsilon_{n+1}\equiv\epsilon\ll 1$, $\mu^{(n)}_{C12\cdots n}$ and $\mu^{(n+1)}_{C12\cdots nn+1}$ appear globally identical.

However, we are interested in the comparison of the two measures within the set P_ϵ rather than globally. By using Eqs. (5) and (8) we can write

$$\begin{aligned}\delta_{12\cdots n,n+1}(P_\epsilon)&=e^{l'/\tau^{(n+1)}}\mu^{(n+1)}_{C12\cdots nn+1}(O^{-l'}_{12\cdots nn+1}(P_\epsilon))\\&\quad-e^{l'/\tau^{(n)}}\mu^{(n)}_{C12\cdots n}(O^{-l'}_{12\cdots n}(P_\epsilon))\\&\simeq-\mu^{(n)}_{C12\cdots n}(O^{-l'}_{12\cdots n}(P_\epsilon)\cap H_{n+1})\\&\quad+\delta_{12\cdots n,n+1}(O^{-l'}_{12\cdots nn+1}(P_\epsilon)),\end{aligned}\tag{A1}$$

where we have abbreviated $l'\equiv l^{(n)}_{12\cdots n}(H_{n+1},P_\epsilon)$, $\tau^{(n)}\equiv\tau^{(n)}_{12\cdots n}$, and $\tau^{(n+1)}\equiv\tau^{(n+1)}_{12\cdots nn+1}$. In this appendix, we keep this notation. The second line in Eq. (A1) results from the identity $O^{-l'}_{12\cdots n}(P_\epsilon)\equiv(O^{-l'}_{12\cdots n}(P_\epsilon)\cap H_{n+1})\cup O^{-l'}_{12\cdots nn+1}(P_\epsilon)$, and the approximations $e^{l'/\tau^{(n+1)}}\simeq 1$ and $e^{l'/\tau^{(n)}}\simeq 1$. Since $l'\sim-\ln\epsilon$ and $\tau^{(n)}\sim\epsilon^{-D_1}$, these approximations are valid for $\epsilon\ll 1$ [8,7]. D_1 denotes the information dimension of the attractor.

Let us consider the first term in Eq. (A1). We argue that $\mu^{(n)}_{C12\cdots n}(O^{-l'}_{12\cdots n}(P_\epsilon)\cap H_{n+1})$ decreases exponentially fast with the increase of l'. For 1D maps, $O^{-l'}_{12\cdots n}(P_\epsilon)\cap H_{n+1}$ is an interval of approximate width $\sim 2\epsilon\exp(-\lambda_1 l')$. For 2D maps, $O^{-l'}_{12\cdots n}(P_\epsilon)$ is a narrow region which is stretched along the stable direction and squeezed along the unstable one [8]. The intersection $O^{-l'}_{12\cdots n}(P_\epsilon)\cap H_{n+1}$ is roughly a rectangle of length 2ϵ and width $2\epsilon\exp(-\lambda_1 l')$. λ_1 denotes the positive Lyapunov exponent obtained for typical initial conditions on the attractor. If we assume that the c measure is smooth along the unstable manifolds, then we can write $\mu^{(n)}_{C12\cdots n}(O^{-l'}_{12\cdots n}(P_\epsilon)\cap H_{n+1})\sim e^{-\lambda_1 l'}$. Thus, due to the chaoticity of the map O, the first term in Eq. (A1) decreases exponentially fast with the increase of l'.

Let us study the value of $\delta_{12\cdots n,n+1}(O^{-l'}_{12\cdots nn+1}(P_\epsilon))$ in dependence of l'. Let μ_0 denote the measure corresponding to a large number ($N\gg 1$) of randomly distributed points in the phase space. Since we assume that μ_0 converges to the measure $\mu^{(n+1)}_{C12\cdots nn+1}$ after $T\gg 1$ iterates of the map $O_{12\cdots nn+1}$, it is clear that $\mu^{(n+1)}_{C12\cdots nn+1}(O^{-T}_{12\cdots nn+1}(P_\epsilon))-\mu_0(O^{-T}_{12\cdots nn+1}(P_\epsilon))\simeq 0$. However, since $\mu^{(n+1)}_{C12\cdots nn+1}$ and $\mu^{(n)}_{C12\cdots n}$ appear globally identical, the quantity $\delta_{12\cdots n,n+1}(O^{-l'}_{12\cdots nn+1}(P_\epsilon))=\mu^{(n+1)}_{C12\cdots nn+1}(O^{-l'}_{12\cdots nn+1}(P_\epsilon))-\mu^{(n)}_{C12\cdots n}(O^{-l'}_{12\cdots nn+1}(P_\epsilon))\simeq 0$ already for relatively small values of l' (e.g., 5–6 for the tent map).

We support this statement by studying the set $O^{-l'}_{12\cdots nn+1}(P_\epsilon)$ in dependence of l' [7]. For 2D maps, the set $O^{-l'}_{12\cdots nn+1}(P_\epsilon)$ is stretched exponentially fast with the increase of l' along the stable manifolds. Thus, it crosses many of the unstable manifolds that carry both $\mu^{(n)}_{C12\cdots n}$ and $\mu^{(n+1)}_{C12\cdots nn+1}$. For 1D maps, $O^{-l'}_{12\cdots nn+1}(P_\epsilon)$ is made of disjoint intervals. The number of these intervals grows exponentially fast with the increase of l'. Furthermore, they are scattered all over the attractor. Thus, as a consequence of the chaoticity of the map O, the set $O^{-l'}_{12\cdots nn+1}(P_\epsilon)$ becomes more democratic with the increase of l' in a sense that the quantity $\delta_{12\cdots n,n+1}(O^{-l'}_{12\cdots nn+1}(P_\epsilon))$ reflects the global agreement between the two measures. In other words, insofar as l' is not small, $\delta_{12\cdots n,n+1}(O^{-l'}_{12\cdots nn+1}(P_\epsilon))\simeq 0$.

We must note that although the map $O_{12\cdots nn+1}$ is (transiently) chaotic, it is sometimes possible that the set $O^{-l'}_{12\cdots nn+1}(P_\epsilon)$ does not stretch exponentially fast along the stable manifolds. If O is a 1D map, it is possible that the number of preimages that $O^{-l'}_{12\cdots nn+1}(P_\epsilon)$ is made of does not grow exponentially fast. This occurs when $O^{-l'}_{12\cdots nn+1}(P_\epsilon)\equiv\emptyset$. (This is very unlikely since $\epsilon\ll 1$.) In this case, the above arguments concerning the set $O^{-l'}_{12\cdots nn+1}(P_\epsilon)$ do not apply. However, in this case $\mu^{(n)}_{C12\cdots n}(O^{-l'}_{12\cdots nn+1}(P_\epsilon))=0$ and $\mu^{(n+1)}_{C12\cdots nn+1}(O^{-l'}_{12\cdots nn+1}(P_\epsilon))=0$. In other words, in such a case we immediately obtain $\delta_{12\cdots n,n+1}(O^{-l'}_{12\cdots nn+1}(P_\epsilon))=0$.

We conclude that for l' larger than some critical value l_c, the two terms from Eq. (A1) are ≈ 0. This is consistent with the global agreement between the two measures (Fig. 2). The critical value l_c depends on the chaoticity of the map ($\lambda_1>0$). For example, the critical value l_c may be chosen as the smallest integer for which $e^{-\lambda_1 l_c}<0.1$ [7]. The difference between the two measures can be observed only at the positions of a few successive iterates of the added hole H_{n+1} (Fig. 2). If we assume that $l^{(n)}_{12\cdots n}(H_{n+1},O^{-l'}_{12\cdots nn+1}(P_\epsilon))>l_c$, which is almost always valid since $\epsilon\ll 1$, Eq. (10) follows immediately.

[1] E. Ott, C. Grebogi, and J. A. Yorke, Phys. Rev. Lett. **64**, 1196 (1990).

[2] W. L. Ditto, S. N. Rauseo, and M. L. Spano, Phys. Rev. Lett. **65**, 3211 (1990); J. Singer, Y-Z. Wang, and H. H. Bau, *ibid.* **66**, 1123 (1991).

[3] F. Romeiras, C. Grebogi, E. Ott, and W. P. Dayawansa, Physica D **58**, 165 (1992); D. Auerbach, C. Grebogi, E. Ott, and J. A. Yorke, Phys. Rev. Lett. **69**, 3479 (1992); T. Shinbrot,

C. Grebogi, E. Ott, and J. A. Yorke, Nature (London) **363**, 411 (1993).
[4] U. Dressler and G. Nitsche, Phys. Rev. Lett. **68**, 1 (1992); P. M. Alsing, A. Gavrielides, and V. Kovanis, Phys. Rev. E **50**, 1968 (1994).
[5] A. Duchâteau, N. P. Bradshaw, and H. Bersini, Int. J. Control **72**, 727 (1999).
[6] E. Ott, *Chaos in Dynamical Systems* (Cambridge University Press, Cambridge, England, 1993).
[7] V. Paar and H. Buljan, Phys. Rev. E **62**, 4869 (2000).
[8] T. Shinbrot, E. Ott, C. Grebogi, and J. A. Yorke, Phys. Rev. Lett. **65**, 3215 (1990).
[9] T. Shinbrot, W. Ditto, C. Grebogi, E. Ott, M. Spano, and J. A. Yorke, Phys. Rev. Lett. **68**, 2863 (1992); T. Shinbrot, E. Ott, C. Grebogi, and J. A. Yorke, Phys. Rev. A **45**, 4165 (1992); E. J. Kostelich, C. Grebogi, E. Ott, and J. A. Yorke, Phys. Rev. E **47**, 305 (1993).
[10] J. P. Eckmann and D. Ruelle, Rev. Mod. Phys. **57**, 617 (1985).
[11] D. Auerbach, P. Cvitanović, J. P. Eckmann, G. Gunaratne, and I. Procaccia, Phys. Rev. Lett. **58**, 2387 (1987).
[12] B. R. Hunt and E. Ott, Phys. Rev. Lett. **76**, 2254 (1996); Phys. Rev. E **54**, 328 (1996).
[13] T. Tél, in *Directions in Chaos*, edited by Hao Bai-lin (World Scientific, Singapore, 1990), Vol. 3, p. 149
[14] T. Tél, Phys. Rev. A **36**, 1502 (1987); P. Szépfalusy and T. Tél, *ibid.* **34**, 2520 (1986); T. Tél, Phys. Lett. A **119**, 65 (1986); H. Lustfeld and P. Szépfalusy, Phys. Rev. E **53**, 5882 (1996); A. Csordás, G. Györgyi, P. Szépfalusy, and T. Tél, Chaos **3**, 31 (1993).
[15] Mukeshwar Dhamala and Y-C. Lai, Phys. Rev. E **60**, 6176 (1999).
[16] P. Gaspard and J. R. Dorfman, Phys. Rev. E **52**, 3525 (1995).
[17] G. Pianigiani and J. A. Yorke, Trans. Am. Math. Soc. **252**, 351 (1979); G. Pianigiani, J. Math. Anal. Appl. **82**, 75 (1981).
[18] N. Chernov and R. Markarian, Bol. Soc. Bras. Math. **28**, 271 (1997); **28**, 315 (1997); N. Chernov, R. Markarian, and S. Troubetzkoy, Ergod. Th. Dynam. Sys. **18**, 1049 (1998); **20**, 1007 (2000).
[19] P. Collet, S. Martinez, and B. Schmitt, Nonlinearity **7**, 1437 (1994); P. Collet, S. Martinez, and V. Maume-Deschamps, *ibid.* **13**, 1263 (2000).
[20] A. Lopes and R. Markarian, SIAM (Soc. Ind. Appl. Math.) J. Appl. Math. **56**, 651 (1996).
[21] C. Grebogi, E. Ott, and J. A. Yorke, Phys. Rev. Lett. **57**, 1284 (1986); C. Grebogi, E. Ott, F. Romeiras, and J. A. Yorke, Phys. Rev. A **36**, 5365 (1987).
[22] The term shadowing is used in many areas of physics. An important issue in nonlinear dynamics is to see whether a certain system (or class of systems) has a shadowing property. In chaotic systems, a numerical trajectory diverges exponentially fast from the true trajectory. Shadowing property of a chaotic system means that there exists a true trajectory with slightly different initial condition that stays close or shadows the numerical trajectory, e.g., see S. M. Hammel, J. A. Yorke, and C. Grebogi, J. Complexity **3**, 136 (1987). We use the term shadowing in connection with rather different phenomena.
[23] V. Paar and N. Pavin, Phys. Rev. E **55**, 4112 (1997).
[24] V. Paar and N. Pavin, Phys. Lett. A **235**, 139 (1997).
[25] E. Bollt, Y-C. Lai, and C. Grebogi, Phys. Rev. Lett. **79**, 3787 (1997); J. Jacobs, E. Ott, and B. R. Hunt, Phys. Rev. E **57**, 6577 (1998); E. Bollt and Y-C. Lai, *ibid.* **58**, 1724 (1998); K. Zyczkowski and E. M. Bollt, Physica D **132**, 392 (1999); Y-C. Lai, E. Bollt, and C. Grebogi, Phys. Lett. A **255**, 75 (1999).
[26] P. Cvitanović, G. H. Gunaratne, and I. Procaccia, Phys. Rev. A **38**, 1503 (1988).
[27] P. Grassberger and I. Proccacia, Phys. Rev. A **28**, 2591 (1983); J. P. Eckmann and I. Proccacia, *ibid.* **34**, 659 (1986).
[28] M. Hénon, Commun. Math. Phys. **50**, 69 (1976).